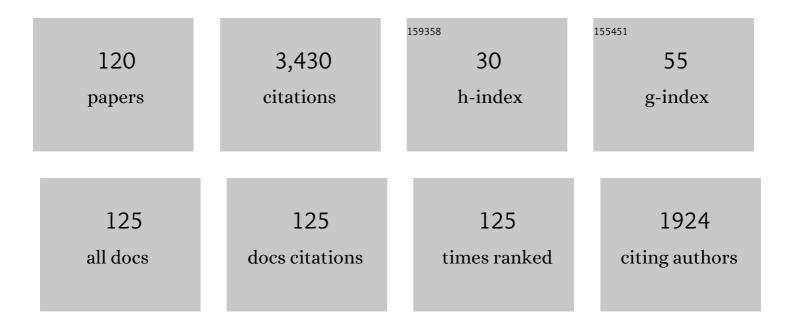
J Gregory Shellnutt

List of Publications by Year in descending order

Source: https://exaly.com/author-pdf/8277104/publications.pdf Version: 2024-02-01



#	Article	IF	CITATIONS
1	The Emeishan large igneous province: A synthesis. Geoscience Frontiers, 2014, 5, 369-394.	4.3	292
2	Permian peralkaline, peraluminous and metaluminous A-type granites in the Panxi district, SW China: Their relationship to the Emeishan mantle plume. Chemical Geology, 2007, 243, 286-316.	1.4	275
3	Precise age determination of mafic and felsic intrusive rocks from the Permian Emeishan large igneous province (SW China). Gondwana Research, 2012, 22, 118-126.	3.0	214
4	The role of Fe–Ti oxide crystallization in the formation of A-type granitoids with implications for the Daly gap: An example from the Permian Baima igneous complex, SW China. Chemical Geology, 2009, 259, 204-217.	1.4	130
5	Formation of the Late Permian Panzhihua plutonic-hypabyssal-volcanic igneous complex: Implications for the genesis of Fe–Ti oxide deposits and A-type granites of SW China. Earth and Planetary Science Letters, 2010, 289, 509-519.	1.8	117
6	Zircon Lu–Hf isotopic compositions of metaluminous and peralkaline A-type granitic plutons of the Emeishan large igneous province (SW China): Constraints on the mantle source. Journal of Asian Earth Sciences, 2009, 35, 45-55.	1.0	101
7	Cretaceous ongonites (topaz-bearing albite-rich microleucogranites) from Ongon Khairkhan, Central Mongolia: Products of extreme magmatic fractionation and pervasive metasomatic fluid: rock interaction. Lithos, 2015, 236-237, 173-189.	0.6	100
8	Elemental and Sr–Nd isotope geochemistry of microgranular enclaves from peralkaline A-type granitic plutons of the Emeishan large igneous province, SW China. Lithos, 2010, 119, 34-46.	0.6	99
9	Flood basalt-related Fe–Ti oxide deposits in the Emeishan large igneous province, SW China. Lithos, 2010, 119, 123-136.	0.6	94
10	Origin of Late Permian Emeishan basaltic rocks from the Panxi region (SW China): Implications for the Ti-classification and spatial–compositional distribution of the Emeishan flood basalts. Journal of Volcanology and Geothermal Research, 2011, 199, 85-95.	0.8	91
11	Formation of Cretaceous Cordilleran and post-orogenic granites and their microgranular enclaves from the Dalat zone, southern Vietnam: Tectonic implications for the evolution of Southeast Asia. Lithos, 2013, 182-183, 229-241.	0.6	91
12	Petrogenesis of the flood basalts from the Early Permian Panjal Traps, Kashmir, India: Geochemical evidence for shallow melting of the mantle. Lithos, 2014, 204, 159-171.	0.6	89
13	No link between the Panjal Traps (Kashmir) and the Late Permian mass extinctions. Geophysical Research Letters, 2011, 38, n/a-n/a.	1.5	82
14	Longevity of the Permian Emeishan mantle plume (SW China): 1 Ma, 8 Ma or 18 Ma?. Geological Magazine, 2008, 145, 373-388.	0.9	72
15	Magmatic duration of the Emeishan large igneous province: Insight from northern Vietnam. Geology, 2020, 48, 457-461.	2.0	70
16	Crustally-derived granites in the Panzhihua region, SW China: Implications for felsic magmatism in the Emeishan large igneous province. Lithos, 2011, 123, 145-157.	0.6	67
17	Three Fe-Ti oxide ore-bearing gabbro-granitoid complexes in the Panxi region of the Permian Emeishan large igneous province, SW China. Numerische Mathematik, 2011, 311, 773-812.	0.7	67
18	Origin of the silicic volcanic rocks of the Early Permian Panjal Traps, Kashmir, India. Chemical Geology, 2012, 334, 154-170.	1.4	62

#	Article	IF	CITATIONS
19	Zircon U–Pb ages and Hf isotopic compositions of alkaline silicic magmatic rocks in the Phan Si Pan-Tu Le region, northern Vietnam: Identification of a displaced western extension of the Emeishan Large Igneous Province. Journal of Asian Earth Sciences, 2015, 97, 102-124.	1.0	57
20	Permian, rifting related fayalite syenite in the Panxi region, SW China. Lithos, 2008, 101, 54-73.	0.6	54
21	Timing of collisional and post-collisional Pan-African Orogeny silicic magmatism in south-central Chad. Precambrian Research, 2017, 301, 113-123.	1.2	45
22	A 1.88†Ga giant radiating mafic dyke swarm across southern India and Western Australia. Precambrian Research, 2018, 308, 58-74.	1.2	45
23	Petrogenesis of the 723 Ma Coronation sills, Amundsen basin, Arctic Canada: implications for the break-up of Rodinia. Precambrian Research, 2004, 129, 309-324.	1.2	44
24	Multiple mantle sources of the Early Permian Panjal Traps, Kashmir, India. Numerische Mathematik, 2015, 315, 589-619.	0.7	42
25	Mineralogy from three peralkaline granitic plutons of the Late Permian Emeishan large igneous province (SW China): evidence for contrasting magmatic conditions of A-type granitoids. European Journal of Mineralogy, 2011, 23, 45-61.	0.4	39
26	Correlation between magmatism of the Ladakh Batholith and plate convergence rates during the India–Eurasia collision. Gondwana Research, 2014, 26, 1051-1059.	3.0	38
27	Petrogenesis of Late Permian silicic rocks of Tu Le basin and Phan Si Pan uplift (NW Vietnam) and their association with the Emeishan large igneous province. Journal of Asian Earth Sciences, 2015, 109, 1-19.	1.0	37
28	A petrogenetic relationship between 2.37†Ga boninitic dyke swarms of the Indian Shield: Evidence from the Central Bastar Craton and the NE Dharwar Craton. Gondwana Research, 2019, 69, 193-211.	3.0	33
29	Petrogenetic implications of mineral chemical data for the Permian Baima igneous complex, SW China. Mineralogy and Petrology, 2012, 106, 75-88.	0.4	32
30	Oxidation zonation within the Emeishan large igneous province: Evidence from mantle-derived syenitic plutons. Journal of Asian Earth Sciences, 2012, 54-55, 31-40.	1.0	32
31	The initial break-up of Pangæa elicited by Late Palæozoic deglaciation. Scientific Reports, 2016, 6, 31442.	1.6	31
32	The Panjal Traps. Geological Society Special Publication, 2018, 463, 59-86.	0.8	30
33	The origin of Late Ediacaran post-collisional granites near the Chad Lineament, Saharan Metacraton, South-Central Chad. Lithos, 2018, 304-307, 450-467.	0.6	29
34	Platinum element group variations at the Permo–Triassic boundary in Kashmir and British Columbia and their significance. Chemical Geology, 2010, 272, 12-19.	1.4	28
35	Origin of peralkaline granites of the Jurassic Bokan Mountain complex (southeastern Alaska) hosting rare metal mineralization. International Geology Review, 2016, 58, 1-13.	1.1	28
36	Petrogenesis of the 1.85†Ga Sonakhan mafic dyke swarm, Bastar Craton, India. Lithos, 2019, 334-335, 88-101.	0.6	26

#	Article	IF	CITATIONS
37	A lower crust origin of some flood basalts of the Emeishan large igneous province, SW China. Journal of Asian Earth Sciences, 2015, 109, 74-85.	1.0	25
38	Petrological modeling of basaltic rocks from Venus: A case for the presence of silicic rocks. Journal of Geophysical Research E: Planets, 2013, 118, 1350-1364.	1.5	24
39	Mantle Exhumation in an Early Paleozoic Passive Margin, Northern Cordillera, Yukon. Journal of Geology, 2003, 111, 313-327.	0.7	23
40	High-Mg andesite genesis by upper crustal differentiation. Journal of the Geological Society, 2010, 167, 1081-1088.	0.9	22
41	Petrogenesis of the Mesoproterozoic (1.23ÂGa) Sudbury dyke swarm and its questionable relationship to plate separation. International Journal of Earth Sciences, 2012, 101, 3-23.	0.9	22
42	Mantle Potential Temperature Estimates and Primary Melt Compositions of the Low-Ti Emeishan Flood Basalt. Frontiers in Earth Science, 2018, 6, .	0.8	21
43	Cryptic regional magmatism in the southern Saharan Metacraton at 580†Ma. Precambrian Research, 2019, 332, 105398.	1.2	20
44	Temporal and structural evolution of the Early Palæogene rocks of the Seychelles microcontinent. Scientific Reports, 2017, 7, 179.	1.6	19
45	Microcontinents among the accretionary complexes of the Central Asia Orogenic Belt: In situ Re–Os evidence. Journal of Asian Earth Sciences, 2013, 62, 37-50.	1.0	16
46	Late Neoproterozoic to Carboniferous genesis of A-type magmas in Avalonia of northern Nova Scotia: repeated partial melting of anhydrous lower crust in contrasting tectonic environments. International Journal of Earth Sciences, 2018, 107, 587-599.	0.9	16
47	Mantle source heterogeneity of the Early Jurassic basalt of eastern North America. International Journal of Earth Sciences, 2018, 107, 1033-1058.	0.9	14
48	Secular isotopic variation in lithospheric mantle through the Variscan orogen: Neoproterozoic to Cenozoic magmatism in continental Europe. Geology, 2019, 47, 637-640.	2.0	14
49	Late Permian mafic rocks identified within the Doba basin of southern Chad and their relationship to the boundary of the Saharan Metacraton. Geological Magazine, 2015, 152, 1073-1084.	0.9	13
50	Linking rock age and soil cover across four islands on the Galápagos archipelago. Journal of South American Earth Sciences, 2020, 99, 102500.	0.6	13
51	Generation of calc-alkaline andesite of the Tatun volcanic group (Taiwan) within an extensional environment by crystal fractionation. International Geology Review, 2014, 56, 1156-1171.	1.1	12
52	Resolving discordant U–Th–Ra ages: constraints on petrogenetic processes of recent effusive eruptions at Tatun Volcano Group, northern Taiwan. Geological Society Special Publication, 2015, 422, 175-188.	0.8	12
53	Generation of felsic rocks of bimodal volcanic suites from thinned and rifted continental margins: Geochemical and Nd, Sr, Pb-isotopic evidence from Haida Gwaii, British Columbia, Canada. Lithos, 2017, 292-293, 146-160.	0.6	12
54	Bokan Mountain peralkaline granitic complex, Alexander terrane (southeastern Alaska): evidence for Early Jurassic rifting prior to accretion with North America. Canadian Journal of Earth Sciences, 2013, 50, 678-691.	0.6	11

#	Article	IF	CITATIONS
55	Evidence of Middle Jurassic magmatism within the Seychelles microcontinent: Implications for the breakup of Gondwana. Geophysical Research Letters, 2015, 42, 10,207.	1.5	11
56	Petrogenesis of the Triassic Bayan-Ulan alkaline granitic pluton in the North Gobi rift of central Mongolia: Implications for the evolution of Early Mesozoic granitoid magmatism in the Central Asian Orogenic Belt. Journal of Asian Earth Sciences, 2015, 109, 50-62.	1.0	11
57	Derivation of intermediate to silicic magma from the basalt analyzed at the Vega 2 landing site, Venus. PLoS ONE, 2018, 13, e0194155.	1.1	11
58	Long-lived association between Avalonia and the Meguma terrane deduced from zircon geochronology of metasedimentary granulites. Scientific Reports, 2019, 9, 4065.	1.6	11
59	An ultramafic primary magma for a low Si, high Ti–Fe gabbro in the Panxi region of the Emeishan large igneous province, SW China. Journal of Asian Earth Sciences, 2014, 79, 329-344.	1.0	10
60	Late Cretaceous intraplate silicic volcanic rocks from the Lake Chad region: An extension of the Cameroon volcanic line?. Geochemistry, Geophysics, Geosystems, 2016, 17, 2803-2824.	1.0	10
61	Petrogenesis of an Eocene syenitic intrusion from south-central British Columbia: Evidence for increasing influence of cratonic Laurentia on alkaline magmatism of western North America. Lithos, 2019, 332-333, 67-82.	0.6	10
62	Neoproterozoic to Cenozoic magmatism in the central part of the Bohemian Massif (Czech Republic): Isotopic tracking of the evolution of the mantle through the Variscan orogeny. Lithos, 2019, 326-327, 358-369.	0.6	10
63	Mantle potential temperature estimates of basalt from the surface of Venus. Icarus, 2016, 277, 98-102.	1.1	9
64	Petrogenetic evolution of Late Paleozoic rhyolites of the Harvey Group, southwestern New Brunswick (Canada) hosting uranium mineralization. Contributions To Mineralogy and Petrology, 2016, 171, 1.	1.2	9
65	Variable magma reservoir depths for Tongariro Volcanic Complex eruptive deposits from 10,000Âyears to present. Bulletin of Volcanology, 2017, 79, 1.	1.1	9
66	Derivation of the Early Carboniferous Wedgeport pluton by crystal fractionation of a mafic parental magma: a rare case of an A-type granite within the Meguma terrane (Nova Scotia, Canada). Geological Magazine, 2020, 157, 248-262.	0.9	9
67	Two series of Ediacaran collision-related granites in the Guéra Massif, South-Central Chad: Tectonomagmatic constraints on the terminal collision of the eastern Central African Orogenic Belt. Precambrian Research, 2020, 347, 105823.	1.2	9
68	An evaluation of crustal assimilation within the Late Devonian South Mountain Batholith, SW Nova Scotia. Geological Magazine, 2012, 149, 353-365.	0.9	8
69	The 186 Ma Dashibalbar alkaline granitoid pluton in the north-Gobi Rift of central Mongolia: Evidence for melting of Neoproterozoic basement above a plume. Numerische Mathematik, 2014, 314, 613-648.	0.7	8
70	Granodiorites of the South Mountain Batholith (Nova Scotia, Canada) derived by partial melting of Avalonia granulite rocks beneath the Meguma terrane: Implications for the heat source of the Late Devonian granites of the Northern Appalachians. Tectonophysics, 2015, 655, 206-212.	0.9	8
71	The curious case of the rock at Venera 8. Icarus, 2019, 321, 50-61.	1.1	8
72	Petrogenesis of post-collisional Late Paleozoic volcanic rocks of the Bohemian Massif (Central) Tj ETQq0 0 0 rgBT	/Overlock 0.6	10 Tf 50 67 8

354-355, 105331.

#	Article	IF	CITATIONS
73	Petrogenesis of the Cenozoic alkaline volcanic rock series of the ÄŒeské StÅ™edohoÅ™Ã-Complex (Bohemian) Ţį ĔTŐd1	1 0.78431
74	Age and tectonic setting of the East Taiwan Ophiolite: implications for the growth and development of the South China Sea. Geological Magazine, 2017, 154, 441-455.	0.9	7
75	An autochthonous Avalonian basement source for the latest Ordovician Brenton Pluton in the Meguma terrane of Nova Scotia: U–Pb–Hf isotopic constraints and paleogeographic implications. International Journal of Earth Sciences, 2018, 107, 955-969.	0.9	7
76	Evidence of silicate immiscibility within flood basalts from the Central Atlantic Magmatic Province. Geochemistry, Geophysics, Geosystems, 2013, 14, 4921-4935.	1.0	6
77	Nd–Sr isotopic constraint to the formation of metatexite and diatexite migmatites, Higo metamorphic terrane, central Kyushu, Japan. International Geology Review, 2016, 58, 405-423.	1.1	6
78	A mineralogical investigation of the Late Permian Doba gabbro, southern Chad: Constraints on the parental magma conditions and composition. Journal of African Earth Sciences, 2016, 114, 13-20.	0.9	6
79	Late Jurassic Leucogranites of Macau (SE China): A Record of Crustal Recycling During the Early Yanshanian Orogeny. Frontiers in Earth Science, 2020, 8, .	0.8	6
80	Geochemistry of continental alkali basalts in the Sabzevar region, northern Iran: implications for the role of pyroxenite in magma genesis. Contributions To Mineralogy and Petrology, 2020, 175, 1.	1.2	6
81	Secular variability of the thermal regimes of continental flood basalts in large igneous provinces since the Late Paleozoic: Implications for the supercontinent cycle. Earth-Science Reviews, 2022, 226, 103928.	4.0	6
82	Old and juvenile source of Paleozoic and Mesozoic basaltic magmas in the Acatlán and Ayð complexes, Southern Mexico: Nd isotopic constraints. Tectonophysics, 2016, 681, 376-384.	0.9	5
83	Mid-Miocene (post 12 Ma) displacement along the central Karakoram fault zone in the Nubra Valley, Ladakh, India from spot LA-ICPMS U/Pb zircon ages of granites. Journal of the Geological Society of India, 2017, 89, 231-239.	0.5	5
84	Silurian U Pb zircon intrusive ages for the Red River anorthosite (northern Cape Breton Island): Implications for the Laurentia-Avalonia boundary in Atlantic Canada. Gondwana Research, 2019, 73, 54-64.	3.0	5
85	An Assessment of the Magmatic Conditions of Late Neoproterozoic Collisional and Post-collisional Granites From the Guéra Massif, South-Central Chad. Frontiers in Earth Science, 2020, 8, .	0.8	5
86	Linking the Wrangellia flood basalts to the Galápagos hotspot. Scientific Reports, 2021, 11, 8579.	1.6	5
87	Late Ediacaran post-collisional magmatism in the Guéra Massif, South-Central Chad. International Geology Review, 0, , 1-22.	1.1	5
88	lgneous Rock Associations 21. The Early Permian Panjal Traps of the Western Himalaya. Geoscience Canada, 2016, 43, 251.	0.3	5
89	Chemical and Sr-Nd compositions and 40Ar/39Ar ages of NW-trending dolerite dikes of Burkina Faso: Evidence for a Mesoproterozoic magmatism in the West African Craton. Geoscience Frontiers, 2018, 9, 1957-1980.	4.3	4
90	Magmatic Sulfide and Fe-Ti Oxide Deposits Associated With Mafic-Ultramafic Intrusions in China. , 2018,		4

, 239-267.

#	Article	IF	CITATIONS
91	Formation of Anorthositic Rocks within the Blair River Inlier of Northern Cape Breton Island, Nova Scotia (Canada). Lithosphere, 2020, 2020, .	0.6	4
92	Petrogenesis of silicic rocks from the Phan Si Pan–Tu Le region of the Emeishan large igneous province, northwestern Vietnam. Geological Society Special Publication, 0, , SP518-2020-253.	0.8	4
93	A cumulate syenite in the upper part of the Hongge-layered mafic–ultramafic intrusion, Emeishan large igneous province, SW China. International Journal of Earth Sciences, 2021, 110, 2979-3000.	0.9	4
94	Chevkinite-group minerals from the mantle-derived metaluminous Woshui syenite of the Emeishan large igneous province. European Journal of Mineralogy, 2013, 25, 671-682.	0.4	3
95	Haida Gwaii (British Columbia, Canada): a Phanerozoic analogue of a subduction-unrelated Archean greenstone belt. Scientific Reports, 2019, 9, 3251.	1.6	3
96	Petrogenesis of Eocene to early Oligocene granitic rocks in Phan Si Pan uplift area, northwestern Vietnam: Geochemical implications for the Cenozoic crustal evolution of the South China Block. Lithos, 2020, 372-373, 105640.	0.6	3
97	Resolving the origin of the Seychelles microcontinent: Insight from zircon geochronology and Hf isotopes. Precambrian Research, 2020, 343, 105725.	1.2	3
98	A petrological experiment on Emeishan basalt: Implications for the formation of syenite from the Baima igneous complex. Terrestrial, Atmospheric and Oceanic Sciences, 2021, 32, 319-338.	0.3	3
99	Modeling results for the composition and typology of non-primary venusian anorthosite. Icarus, 2021, 366, 114531.	1.1	3
100	Mantle Potential Temperature Estimates of Basalt from the East Taiwan Ophiolite. Terrestrial, Atmospheric and Oceanic Sciences, 2016, 27, 853-863.	0.3	3
101	Climatic fluctuations during a mass extinction: Rapid carbon and oxygen isotope variations across the Permian-Triassic (PTr) boundary at Guryul Ravine, Kashmir, India. Journal of Asian Earth Sciences, 2022, 227, 105066.	1.0	3
102	Platinum-group elemental chemistry of the Baima and Taihe Fe–Ti oxide bearing gabbroic intrusions of the Emeishan large igneous province, SW China. Chemie Der Erde, 2015, 75, 35-49.	0.8	2
103	Rapid determination of initial 87Sr/86Sr and estimation of the Rb-Sr age of plutonic rocks by LA-ICPMS of variably altered feldspars: An example from the 1.14†Ga Great Abitibi Dyke, Ontario, Canada. Lithos, 2018, 314-315, 52-58.	0.6	2
104	Tectonomagmatic development of the Eocene Pasevh pluton (NW Iran): Implications for the Arabia-Eurasia collision. Journal of Asian Earth Sciences, 2020, 203, 104551.	1.0	2
105	The enigmatic continental crust of North-Central Africa: Saharan Metacraton or Central Sahara Shield?. South African Journal of Geology, 2021, 124, 383-390.	0.6	2
106	Insight into crustal contamination and hydrothermal alteration of the Panjal Traps (Kashmir) from O-isotopes. International Geology Review, 2022, 64, 1556-1573.	1.1	2
107	Editorial: Granite Petrogenesis and Geodynamics. Frontiers in Earth Science, 2021, 8, .	0.8	2
108	Eocene Volcanic Complex from Central British Columbia: The Role of Fractional Crystallization during the Magmatic Evolution. Lithosphere, 2022, 2022, .	0.6	2

#	Article	IF	CITATIONS
109	Platinum-group element geochemistry of the Panjal Traps: constraints on mantle melting and implications for mineral exploration. Geological Society Special Publication, 0, , SP518-2020-241.	0.8	1
110	DERIVATION OF THE EARLY CARBONIFEROUS WEDGEPORT PLUTON BY CRYSTAL FRACTIONATION OF A MAFIC PARENTAL MAGMA: A RARE CASE OF AN A-TYPE GRANITE WITHIN THE MEGUMA TERRANE (NOVA SCOTIA,) TJ ETC	Qq0 0 0 rg	BI /Overlock
111	Platinum-Group Element Geochemistry of Boradih Ultramafic Intrusion from the Sonakhan Greenstone Belt, Bastar Craton. , 2020, , .		1
112	Magmatic and Inherited Zircon Ages from a Diorite Xenolith of the Popes Harbour Dyke, Nova Scotia: Implications for Late Ediacaran Arc Magmatism in the Avalon Terrane of the Northern Appalachians. Minerals (Basel, Switzerland), 2022, 12, 575.	0.8	1
113	Perspectives on lithospheric evolution through tectonomagmatic processes: a volume in honour of Jaroslav Dostal—an introduction. International Journal of Earth Sciences, 2018, 107, 781-785.	0.9	0
114	Platinumâ€group element and Au geochemistry of an ultramafic intrusion from the Sonakhan greenstone belt, Bastar craton, Central India: Tectonoâ€magmatic implications. Geological Journal, 0, , .	0.6	0
115	Igneous Rock Associations 16. The Late Permian Emeishan Large Igneous Province. Geoscience Canada, 2015, 42, 169-180.	0.3	0
116	LATE NEOPROTEROZOIC TO CARBONIFEROUS GENESIS OF A-TYPE MAGMAS IN AVALONIA OF NORTHERN NOVA SCOTIA: REPEATED PARTIAL MELTING OF ANHYDROUS LOWER CRUST IN CONTRASTING TECTONIC ENVIRONMENTS. , 2017, , .		0
117	AGE AND FORMATION OF ANORTHOSITIC ROCKS WITHIN THE BLAIR RIVER INLIER OF NORTHERN CAPE BRETON ISLAND, NOVA SCOTIA (CANADA). , 2019, , .		0
118	Late Ediacaran post-collisional magmatism in the Gu $ ilde{A}$ ©ra Massif, South-Central Chad. , 2021, , .		0
110	The formation of tonalitic and granodioritic melt from Venusian basalt. Scientific Reports, 2022, 12,	16	0

120Igneous Rock Associations 28. Construction of a Venusian Greenstone Belt: A Petrological0.30Perspective. Geoscience Canada, 2021, 48, .0.30